The role of ocean thermal expansion in Last Interglacial sea level rise

Nicholas P. McKay,[1] Jonathan T. Overpeck,[1,2,3] and Bette L. Otto-Bliesner[4]

Received 25 May 2011; revised 7 June 2011; accepted 9 June 2011; published 21 July 2011.

[1] A compilation of paleoceanographic data and a coupled atmosphere-ocean climate model were used to examine global ocean surface temperatures of the Last Interglacial (LIG) period, and to produce the first quantitative estimate of the role that ocean thermal expansion likely played in driving sea level rise above present day during the LIG. Our analysis of the paleoclimatic data suggests a peak LIG global sea surface temperature (SST) warming of 0.7 ± 0.6°C compared to the late Holocene. Our LIG climate model simulation suggests a slight cooling of global average SST relative to preindustrial conditions (ΔSST = −0.4°C), with a reduction in atmospheric water vapor in the Southern Hemisphere driven by a northward shift of the Intertropical Convergence Zone, and substantially reduced seasonality in the Southern Hemisphere. Taken together, the model and paleoceanographic data imply a minimal contribution of ocean thermal expansion to LIG sea level rise above present day. Uncertainty remains, but it seems unlikely that thermosteric sea level rise exceeded 0.4 ± 0.3 m during the LIG. This constraint, along with estimates of the sea level contributions from the Greenland Ice Sheet, glaciers and ice caps, implies that 4.1 to 5.8 m of sea level rise during the Last Interglacial period was derived from the Antarctic Ice Sheet. These results reemphasize the concern that both the Antarctic and Greenland Ice Sheets may be more sensitive to temperature than widely thought. **Citation:** McKay, N. P., J. T. Overpeck, and B. L. Otto-Bliesner (2011), The role of ocean thermal expansion in Last Interglacial sea level rise, *Geophys. Res. Lett.*, *38*, L14605, doi:10.1029/2011GL048280.

1. Introduction

[2] Sea level rise is one of the major socio-economic hazards associated with global warming, and a better understanding the mechanisms that underlie sea level rise is a prerequisite to accurate projections of global and regional sea level rise. Despite this, variability in the different components of sea level rise (i.e., ocean thermal expansion, melting of glaciers, and wasting of the Greenland and Antarctic Ice Sheets) is poorly understood, especially with respect to the future. The Fourth Assessment Report of the Intergovernmental Panel on Climate Change (IPCC), which explicitly excluded rapid ice flow dynamics, projected that ocean thermal expansion would make up 55 to 70% of the sea level rise over the 21st century [*Meehl et al.*, 2007], whereas the empirical model of *Vermeer and Rahmstorf* [2009] projects a much smaller proportion, between 20 and 30%, although this result is primarily driven by a larger contribution of ice melt. On longer timescales, the equilibrium response of ocean thermal expansion to warming has been estimated as 0.2 to 0.6 m $°C^{-1}$ [*Meehl et al.*, 2007], but the relative contributions of ice sheet melt and thermal expansion during a millennial-scale highstand remains unclear. One approach to address this uncertainty is to study past sea level changes. The last interglacial period (LIG) is the most recent warm interval with substantially higher-than-modern global sea level. During the LIG, from ca. 130 to 120 ka, sea level reached at least 6 m above present levels [*Hearty et al.*, 2007; *Kopp et al.*, 2009]. The majority of the sea level rise originated from melting of the Greenland Ice Sheet (GIS) and the Antarctic Ice Sheets [*Otto-Bliesner et al.*, 2006; *Overpeck et al.*, 2006; *Kopp et al.*, 2009; *Clark and Huybers*, 2009], but the role of thermal expansion has not been carefully examined. Here, we compile the available paleoceanographic records and examine global climate model simulations to better constrain the amount of thermal expansion during the LIG.

2. Methods

2.1. Paleoclimate Data

[3] We compiled a dataset of 76 published sea surface temperature (SST) records that met several criteria. Only quantitative SST records that included both the LIG and the Holocene were included so that ΔSST values (warmest LIG – late Holocene) could be calculated internally for each record. We restricted our analyses to records that had an average temporal resolution of 3 kyr or better during both LIG and the Holocene. Records were obtained through the NOAA Paleoclimatology World Data Center (www.ngdc.noaa.gov/paleo/paleo.html), the Pangaea database (www.pangaea.de), and from individual site reports and papers (auxiliary material, Table S1).[1] The sea surface temperatures (SSTs) were determined using Mg/Ca ratios in foraminifera, alkenone unsaturation ratios (i.e., U^{k}_{37}), and faunal assemblage transfer functions (for radiolaria, foraminifera, diatoms and coccoliths), and were interpreted to reconstruct annual, austral summer, and boreal summer sea surface temperatures. Only records with published age models were included; however, there is substantial uncertainty between age estimates at different sites. For this study we chose to determine a *maximum* estimate of ocean warming during a sustained sea level highstand, so the average SST of a 5 kyr period centered on the warmest

[1]Department of Geosciences, University of Arizona, Tucson, Arizona, USA.
[2]Institute of the Environment, University of Arizona, Tucson, Arizona, USA.
[3]Department of Atmospheric Science, University of Arizona, Tucson, Arizona, USA.
[4]National Center for Atmospheric Research, Boulder, Colorado, USA.

0094-8276/11/2011GL048280

[1]Auxiliary materials are available in the HTML. doi:10.1029/2011GL048280.

temperature between 135 and 118 ka was calculated for each record. ΔSST values were determined by subtracting the average SST of the late Holocene (5 to 0 ka) from the 5 kyr LIG average. The data set was supplemented by 94 LIG SST estimates from the CLIMAP project [*CLIMAP Project Members*, 1984]. For the CLIMAP data, ΔSST values were determined as the difference between LIG temperatures and core top temperature estimates at each site. Global mean SST anomalies (ΔSST) were calculated by averaging anomalies in 10° × 10° boxes, then determining zonal averages, which were finally averaged after weighting each zonal average by the area of ocean for each latitudinal band.

[4] To complement our data synthesis, we performed the same analyses on the LIG SST dataset assembled by *Turney and Jones* [2010]. The *Turney and Jones* [2010] dataset differs from our synthesis in several regards: 1) only data that were interpreted to reconstruct annual mean temperatures were included, 2) the timing of LIG mean SST estimates was determined by corresponding marine δ^{18}O records and 3) ΔSST values were calculated as the difference between LIG SSTs and instrumental SST climatology. Many of the same records went into both LIG SST syntheses, but analyzing both datasets allows us to evaluate the sensitivity of our results to markedly different data treatment approaches.

2.2. Global Climate Model Simulations

[5] Climate simulations were conducted using a global, coupled ocean-atmosphere-land-sea ice general circulation model (Community Climate System Model [CCSM], Version 3) [*Collins et al.*, 2006]. The atmospheric model has ~1.4° latitude-longitude resolution (T85) with 26 levels, and the ocean model has ~1° resolution and 40 levels. The preindustrial 1870 AD control simulation includes the appropriate forcing conditions, including trace gas concentrations (CO_2: 289 ppmv; CH_4 901 ppbv), solar constant (1365 W/m^2), and orbital characteristics (obliquity: 23.44°, perihelion: 3 January, and eccentricity: 0.0167). The preindustrial control simulation was run for 550 model years, and climatologies were calculated using model years 530 to 549. The LIG simulation included forcing conditions appropriate for 125 ka; obliquity was 23.80°, perihelion was 23 July, and eccentricity was 0.0400 [*Berger and Loutre*, 1991]. The trace gas concentrations were estimated from ice core data (CO_2: 273 ppmv; CH_4: 642 ppbv) [*Petit et al.*, 1999]. The solar constant was set to the model present-day value of 1367 W/m^2. Vegetation and land ice coverage were prescribed at their present-day distributions for both the preindustrial and LIG simulations. The LIG simulation was run for 200 model years, and climatologies were calculated using model years 180 to 199. CCSM3 is known to have regional SST biases, but is very well-suited for simulating global mean SST [*Collins et al.*, 2006], which is the focus of this study. Global SST anomalies were calculated by zonal averaging and then calculating an area-weighted global mean.

3. Paleoceanographic Data Synthesis

[6] LIG-Holocene SST anomalies varied regionally, and importantly, were not uniformly warmer during the LIG (Figure 1). Furthermore, our data synthesis shows the same primary patterns as the synthesis of *Turney and Jones* [2010], suggesting that the primary results are robust to the choices of averaging and Holocene reference period. Records from the high latitudes of the Northern Hemisphere (>30°N) were consistently warmer during the LIG. This is consistent with the dramatic increase in summer insolation (~12% above preindustrial), and extensive evidence for much warmer (4–5°C) conditions in the Arctic during the interval [*CAPE Project Members*, 2006]. South of ~30°N, the anomalies are regionally variable (Figure 1). The Caribbean Sea and the tropical Atlantic Oceans appear to have been generally cooler during the LIG than the late Holocene (and late 20th century). The eastern equatorial Pacific Ocean shows both positive and negative anomalies, as does the rest of the Pacific Ocean. The western Indian Ocean appears to have been slightly warmer, and the central Indian Ocean somewhat cooler, but the data coverage in both the Pacific and Indian Ocean is poor. The southeastern Atlantic Ocean, off the west coast of South Africa, was consistently warmer. The Southern Ocean changes are mixed, apparently cooler west of South America, somewhat warmer in the Atlantic sector and near New Zealand, and mixed in the Indian sector.

[7] The regional variability is interesting, and warrants further investigation, however interpreting the patterns in terms of modes of climatic and ocean variability is confounded by chronological errors, resolution differences and poor data coverage. Consequently, we chose to focus on the primary, global pattern: the warmer temperatures between 30°N and 70°N, and equivocal anomalies further south (Figure 1). The ocean-area-weighted global average SST anomaly is 0.7 ± 0.6°C for our data synthesis, and 0.7°C for that of *Turney and Jones* [2010]. Interestingly, these global ΔSST estimates are lower than the global land and ocean temperature anomaly (1.5 ± 0.1°C) calculated by *Turney and Jones* [2010]. This discrepancy may be due to the predominance of terrestrial records from the Northern Hemisphere that are particularly sensitive to summer temperatures in their global synthesis.

[8] The error calculated for global ΔSST incorporates errors in the SST proxies, which typically range from 1 to 2°C, and the error associated with estimating global ΔSST from limited spatial coverage (auxiliary material). Nevertheless, this estimate does not capture all of uncertainty in global ΔSST. Because we calculated a maximum estimate for ΔSST, we excluded chronological errors, although differences in temporal resolution between sites contributes additional uncertainty. Furthermore, each of the SST proxies comes with its own set of errors and biases. A particular concern is that all three of the primary SST proxies in our database (faunal assemblages, Mg/Ca, U^{k}_{37}) are known to be sensitive to changes in seasonality [*Anand et al.*, 2003; *Morey et al.*, 2005; *Lorenz et al.*, 2006], and each proxy may exhibit different responses to changes in seasonality, even at the same location [e.g., *Weldeab et al.*, 2007; *Saher et al.*, 2009]. Given the extreme differences in seasonal insolation forcing during the LIG relative to the late Holocene, changes in the timing and distribution of the productive seasons likely biased the SST estimates.

[9] To evaluate some of the potential biases in our analysis, we subsampled our database by proxy type and seasonality (auxiliary material). Globally, ΔSST for the U^{k}_{37} and Mg/Ca proxies was about 1.5°C higher than the faunal assemblage proxies. Some of this offset is likely due to lower sample density and different spatial coverage of the U^{k}_{37} and Mg/Ca proxies, which are commonly located near coasts in upwelling regions. Regionally, ΔSST appears generally consistent

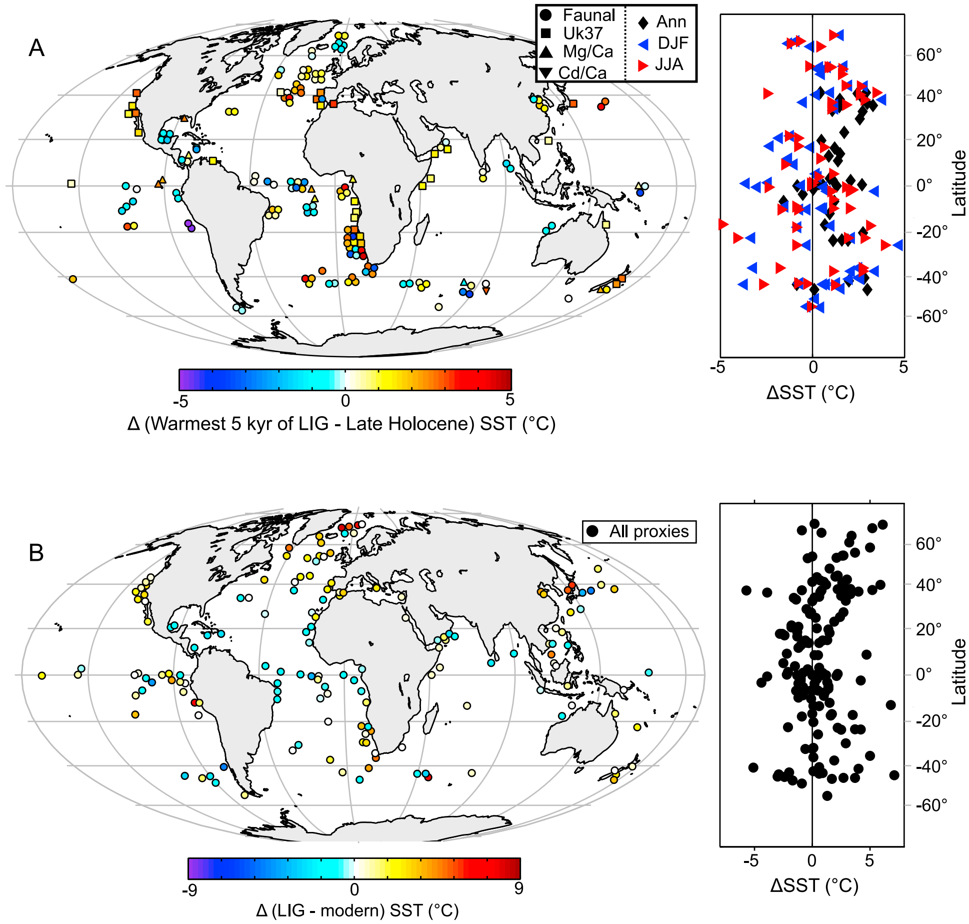

Figure 1. Maps of global ΔSST values in (a) our database, where symbols indicate proxy type (see legend) and (b) the synthesis of *Turney and Jones* [2010]. Note that in both maps, the locations of the symbols were adjusted slightly for visibility. To the right of each map, ΔSST values are plotted by latitude. For our database (Figure 1a), records interpreted to reflect annual, austral summer, and boreal summer temperatures are shown with different symbols.

between proxies, with some exceptions (Figure 1a). Subdividing seasonally, ΔSST in boreal summer (JJA) records was slightly higher (0.2°C) than in austral summer (DJF) records, consistent with the change in insolation forcing.

4. Global Climate Model Simulations

[10] Like the paleoceanographic data, the model simulations for 125 ka show substantial warming north of 40°N, and similar or slightly cooler SSTs south of 30°N (Figures 2a and 2b), similar to previously published simulations for this time period [*Montoya et al.*, 2000; *Kaspar and Cubasch*, 2007]. The ocean-area-weighted global average ocean temperature difference between the 125 ka simulation and the preindustrial control is −0.4°C for both the surface temperatures and the top 200 m. The result of a cooler average ocean surface in the 125 ka simulation is surprising given that the annual insolation anomalies are positive globally (Figure 2c). This result merits a discussion of the climate dynamics simulated in the model that contribute to the cooling in the Southern Hemisphere.

[11] The most significant difference between the forcings for the LIG simulation and the preindustrial control are the different orbital parameters, and among those, the date of perihelion (or phase in the precession cycle) is most different. In the LIG simulation, perihelion occurs during the boreal summer, as opposed to the preindustrial control, when aphelion occurs during the boreal summer. The result is that relative to the preindustrial simulation, the Northern Hemisphere should experience much greater seasonality (warmer summers and colder winters), while the Southern Hemisphere should have colder summers and warmer winters (Figure 2c).

[12] The Southern Hemisphere cooling in the model is associated with a decrease in longwave radiative forcing (Figure 2d), which is a function of decreased water vapor concentrations in the southern hemisphere (Figure 2e). Annually averaged, water vapor content was consistently lower in the LIG simulation than the preindustrial control throughout most of the Southern Hemisphere and over the Pacific Ocean, and substantially higher over the Northern Hemisphere monsoon regions, and the high Northern latitudes (Figure 2e). There appear to be two global scale mechanisms responsible for the hemispheric shift in water vapor.

[13] First, the large increase in summer insolation in the Northern Hemisphere results in a strengthening of the Asian, African and North American Monsoons in the model, along with a northward shift of the Intertropical Convergence Zone (ITCZ) (Figure 2e). The strengthened and northward-

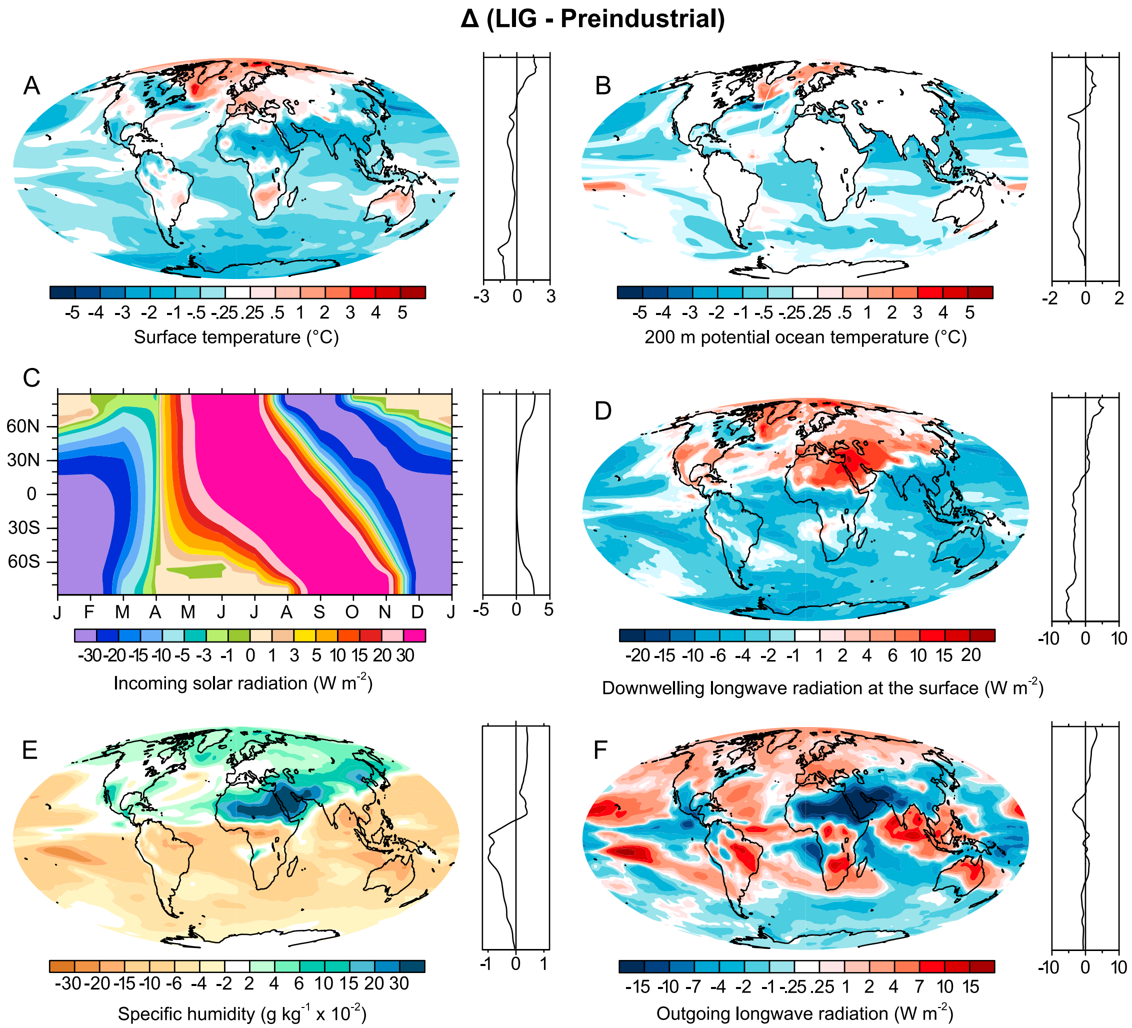

Figure 2. Annual LIG simulation-preindustrial control anomalies in our global climate model simulation parameters. The parameters include: (a) surface air temperature, (b) potential temperature averaged over the top 200 m of the ocean, (c) incoming solar radiation, by latitude and month, (d) downwelling longwave radiation at the surface, (e) specific humidity, averaged over all layers of the atmosphere and (f) outgoing longwave radiation at the top of the model. Zonal average anomalies are plotted to the right of each map.

shifted monsoon systems pull more moisture further across the equator into the Northern Hemisphere, focusing precipitation in the monsoons while effectively drying the southern tropics. The effect of this northward shift on the Earth's energy budget is apparent in the changes in outgoing longwave radiation (OLR) (Figure 2f), which is substantially reduced over the Northern Hemisphere monsoon regions, and increased over the Southern Hemisphere monsoon systems (e.g., South America, equatorial and southern Africa, Australia), effectively cooling the tropical Southern Hemisphere.

[14] The second mechanism is associated with the opposing changes in seasonality in each hemisphere. Due to the nonlinearity in the capacity of air to hold water vapor as a function of temperature (the Clausius-Clapeyron relation), the large decrease in insolation during the Southern Hemisphere summer and fall is not compensated, in terms of specific humidity, by an equivalent increase in winter and spring insolation. This effect should be most important at higher latitudes, and the increase in Northern Hemisphere specific humidity is consistent with this hypothesis (Figure 2e). The impact is not immediately apparent in OLR (Figure 2f). At the high southern latitudes, both downwelling radiation at the surface (Figure 2d) and OLR (Figure 2f) are decreased. This is due to decreased absorption and attenuation of longwave radiation in the atmosphere, and is a function of both decreased specific humidity and cooler surface temperatures decreasing the amount of outgoing longwave radiation produced at the surface. The opposite scenario is apparent at the high northern latitudes.

[15] These two mechanisms provide a plausible explanation for the cooling over most of the world's ocean. The results do not appear to be specific to the CCSM3 model. Simulations with other climate models show cooler temperatures in the Southern Hemisphere, and near-zero or negative annual SST anomalies relative to preindustrial controls [e.g., *Montoya et al.*, 2000; *Kaspar and Cubasch*, 2007]. Furthermore, an additional simulation using CCSM3 for the period 130 ka yields a similar cooling in the Southern Hemisphere, despite regional differences in SST, suggesting that our result is not specific to only this interval of the LIG (auxiliary material). This result calls into question the belief that the LIG was substantially warmer globally [e.g., *LIGA members*, 1991;

Clark and Huybers, 2009; *Turney and Jones*, 2010; *Masson-Delmotte et al.*, 2010]. Much uncertainty remains in model simulations; but it is possible that the predominance of terrestrial, Northern Hemisphere, summer-sensitive temperature proxies may have biased our understanding of global temperature anomalies during the interval.

5. The Thermosteric Component of LIG Sea Level Rise

[16] The amount of steric sea level rise can be determined by calculating the specific volume of the ocean, which requires integrating the temperature and salinity structure of the ocean. This is possible for the model simulations, but not for the paleoceanographic data, so other approaches must be utilized. A simple empirical approach is to estimate a thermal expansion sensitivity (i.e., cm/°C). This can be achieved with instrumental data; the IPCC [*Bindoff et al.*, 2007] concluded that the top 700 m of the ocean warmed 0.1°C from 1961–2003, and that thermal expansion of the ocean was about 1.3 cm over the same interval, resulting in a sensitivity of ~13 cm/°C. To determine a maximum estimate, we assumed our average ΔSST of 0.7 ± 0.6°C is representative of the top 700 m, resulting in 9 ± 8 cm of thermosteric sea level rise. Alternatively, we estimate the thermal expansion using the Thermodynamic Equation of Seawater 2010 (TEOS-10) to calculate the change in the specific volume of the top 700 m of the ocean due to a 0.7 ± 0.6°C warming, while holding the salinity constant, and neglecting changes in ocean area. This approach results in ~12 ± 10 cm of thermosteric sea level rise. It is possible that sustained, warmer-than-modern conditions resulted in warming below 700 m in the oceans. If the average warming extended to 2000 m, the thermal expansion of the ocean would have been about 35 ± 30 cm, consistent with the equilibrium ocean-temperature thermal expansion sensitivity observed in long climate model simulations (0.2 to 0.6 m $°C^{-1}$) [*Meehl et al.*, 2007].

[17] For the model simulation, the whole-ocean global average steric sea level change was −18 cm, primarily due to cooler ocean temperatures in the Southern Hemisphere. Because the model simulations are relatively short, the deep ocean was not equilibrated. This introduces additional uncertainty in our estimate of steric sea level change; however the volume-integrated ocean temperature trends are the same in both the LIG and preindustrial simulations (−0.12°C/century), suggesting that the steric sea level change would be comparable after equilibration.

[18] Altogether, it is clear that ocean thermal expansion during the LIG was a small component of the maximum LIG sea level highstand. A conservative estimate from the available paleoclimatic data is 0.4 ± 0.3 m. The climate model simulations suggest that the thermosteric component may have been smaller or even negative 125 ka, near the time of the maximum highstand. This has several important implications. First the high-end estimate of sea level exceedance (33% probability that sea level exceeded 9.4 m during the LIG) by *Kopp et al.* [2009] is probably too high, because the stochastic thermosteric component in their model was unrealistically large (mean = 0 m, $1\sigma = 2$ m). Using a more realistic thermosteric component should reduce the variance of the distribution of sea level histories, resulting in tighter error estimates and exceedance levels that are nearer to the median.

[19] Secondly, our results provide further constraints on the relative contributions to sea level rise during the last interglacial. The contribution from the GIS was likely 2.2–3.4 m [*Otto-Bliesner et al.*, 2006], or even less [*Oerlemans et al.*, 2006]. The maximum possible contribution from mountain glaciers and ice caps is 0.6 ± 0.1 m [*Radić and Hock*, 2010], and our conservative estimate of maximum thermal expansion during the LIG (0.4 ± 0.3 m). These data, combined with the median projection (50% exceedance) of maximum LIG sea level rise (8.5 m) [*Kopp et al.*, 2009] imply that the Antarctic Ice Sheet (AIS), most likely the West Antarctic Ice Sheet (WAIS), contributed at least 4.1 ± 0.3 m. Assuming a low-end contribution from the GIS (2.2 m), only glaciers and ice caps from the northern Hemisphere (0.4 ± 0.1 m) and our low-end estimate for thermal expansion (0.1 ± 0.1 m), the maximum contribution from Antarctica is 5.8 ± 0.1 m.

[20] It remains unclear why so much more ice (4.1 to 5.8 m sea level equivalent) was lost from Antarctica during the LIG than the Holocene. Antarctic ice cores all suggest warmer-than-modern annual temperatures for East Antarctica [cf. *Petit et al.*, 1999; *EPICA Community Members*, 2004; *Kawamura et al.*, 2007], and recent evidence suggests that the warming anomaly may have been larger (~6°C warmer than the Holocene) than previously estimated [*Sime et al.*, 2009]. This stands in contrast to the cooling simulated by our LIG simulation (Figures 2a and 2b), and is a consistent frustration of model-paleodata comparisons [*Masson-Delmotte et al.*, 2010]. Furthermore, melt season solar insolation was substantially lower than present-day (Figure 2c). A recent study by *Huybers and Denton* [2008] suggested that Antarctic temperatures are primarily controlled by the duration of summer, which was very long during this interval, rather than the intensity of solar insolation (like the Northern Hemisphere), although this mechanism does not drive warmer Antarctic temperatures in our LIG simulation. It has also been hypothesized that poorly simulated climatic feedbacks and changes in ocean circulation may be responsible for the mismatch [*Overpeck et al.*, 2006; *Masson-Delmotte et al.*, 2010], a hypothesis that implies substantial vulnerability of the AIS in the future [*Yin et al.*, 2011]. Finally, it is possible that much of the Antarctic contribution was derived during late deglaciation or early LIG, when melt-season insolation was much higher [*Overpeck et al.*, 2006]. This possibility is consistent with the observation that substantial downwasting of the WAIS is necessary to simulate the high temperatures inferred from East Antarctic ice cores during the LIG in climate models [*Holden et al.*, 2010].

6. Conclusion

[21] The available paleoceanographic records and our LIG GCM simulation suggest that global SSTs were not dramatically warmer than preindustrial conditions (paleodata = 0.7 ± 0.6°C warmer, model = 0.4°C cooler). Taken together, the model and paleodata imply a minimal (−0.2 to 0.4 m) contribution of thermal expansion to LIG sea level rise. This constraint, along with estimates of the sea level contributions from the Greenland Ice Sheet, glaciers and ice caps, implies that 4.1 to 5.8 m of sea level rise during the LIG was derived from the Antarctic Ice Sheet. These results reemphasize the concern that the Greenland and especially the Antarctic Ice Sheets may be more sensitive to temperature than widely thought.

[22] **Acknowledgments.** We thank Suz Tolwinski-Ward, Joellen Russell, John Fasullo, Toby Ault, and Sarah Truebe for insightful discussions on the work presented in this paper. Nan Rosenbloom provided the numbers for the model forcings. NCAR is funded by NSF. We also thank Mark Siddall and Michael Oppenheimer for helpful comments in review of this paper. Computing was done at NCAR as part of the Climate Simulation Laboratory.

[23] The Editor thanks Mark Siddall and Michael Oppenheimer for their assistance in evaluating this paper.

References

Anand, P., H. Elderfield, and M. H. Conte (2003), Calibration of Mg/Ca thermometry in planktonic foraminifera from a sediment trap time series, *Paleoceanography*, *18*(2), 1050, doi:10.1029/2002PA000846.

Berger, A., and M. F. Loutre (1991), Insolation values for the climate of the last 10 million years, *Quat. Sci. Rev.*, *10*, 297–317, doi:10.1016/0277-3791(91)90033-Q.

Bindoff, N., et al. (2007), Observations: Oceanic climate change and sea level, in *Climate Change 2007: The Physical Science Basis. Contribution of Working Group I to the Fourth Assessment Report of the Intergovernmental Panel on Climate Change*, edited by S. Solomon et al., pp. 385–432, Cambridge Univ. Press, Cambridge, U. K.

CAPE Project Members (2006), Last Interglacial Arctic warmth confirms polar amplification of climate change, *Quat. Sci. Rev.*, *25*, 1383–1400, doi:10.1016/j.quascirev.2006.01.033.

Clark, P. U., and P. Huybers (2009), Interglacial and future sea level, *Nature*, *462*, 856–857, doi:10.1038/462856a.

CLIMAP Project Members (1984), The Last Interglacial ocean, *Quat. Res.*, *21*, 123–224, doi:10.1016/0033-5894(84)90098-X.

Collins, W. D., et al. (2006), The Community Climate System Model version 3 (CCSM3), *J. Clim.*, *19*, 2122–2143, doi:10.1175/JCLI3761.1.

EPICA Community Members (2004), Eight glacial cycles from an Antarctic ice core, *Nature*, *429*, 623–628, doi:10.1038/nature02599.

Hearty, P. J., J. T. Hollin, A. Neumann, M. O'Leary, and M. McCulloch (2007), Global sea-level fluctuations during the last interglaciation (MIS 5e), *Quat. Sci. Rev.*, *26*, 2090–2112, doi:10.1016/j.quascirev.2007.06.019.

Holden, P. B., et al. (2010), Interhemispheric coupling, the West Antarctic Ice Sheet and warm Antarctic interglacials, *Clim. Past*, *6*, 431–443, doi:10.5194/cp-6-431-2010.

Huybers, P., and G. Denton (2008), Antarctic temperature at orbital timescales controlled by local summer duration, *Nat. Geosci.*, *1*, 787–792, doi:10.1038/ngeo311.

Kaspar, F., and U. Cubasch (2007), Simulations of the Eemian interglacial and the subsequent glacial inception with a coupled ocean-atmosphere general circulation model, in *The Climate of Past Interglacials*, edited by F. Sirocko et al., pp. 499–515, Elsevier, Boston, Mass.

Kawamura, K., et al. (2007), Northern Hemisphere forcing of climatic cycles in Antarctica over the past 360,000 years, *Nature*, *448*, 912–916, doi:10.1038/nature06015.

Kopp, R., F. J. Simons, J. X. Mitrovica, A. Maloof, and M. Oppenheimer (2009), Probabilistic assessment of sea level during the Last Interglacial stage, *Nature*, *462*, 863–867, doi:10.1038/nature08686.

LIGA members (1991), Report of 1st discussion group: The Last Interglacial in high latitudes of the Northern Hemisphere: Terrestrial and marine evidence, *Quat. Int.*, *10–12*, 9–28, doi:10.1016/1040-6182(91)90038-P.

Lorenz, S. J., J. Kim, N. Rimbu, R. R. Schneider, and G. Lohmann (2006), Orbitally driven insolation forcing on Holocene climate trends: Evidence from alkenone data and climate modeling, *Paleoceanography*, *21*, PA1002, doi:10.1029/2005PA001152.

Masson-Delmotte, V., et al. (2010), EPICA Dome C record of glacial and interglacial intensities, *Quat. Sci. Rev.*, *29*, 113–128, doi:10.1016/j.quascirev.2009.09.030.

Meehl, G. A., et al. (2007), Global climate projections, in *Climate Change 2007: The Physical Science Basis. Contribution of Working Group I to the Fourth Assessment Report of the Intergovernmental Panel on Climate Change*, edited by S. Solomon et al., chap. 10, pp. 747–785, Cambridge Univ. Press, Cambridge, U. K.

Montoya, M., H. von Storch, and T. J. Crowley (2000), Climate simulation for 125 kyr BP with a coupled ocean-atmosphere general circulation model, *J. Clim.*, *13*, 1057–1072, doi:10.1175/1520-0442(2000)013<1057:CSFKBW>2.0.CO;2.

Morey, A. E., A. C. Mix, and N. G. Pisias (2005), Planktonic foraminiferal assemblages preserved in surface sediments correspond to multiple environment variables, *Quat. Sci. Rev.*, *24*, 925–950, doi:10.1016/j.quascirev.2003.09.011.

Oerlemans, J., D. Dahl-Jensen, and V. Masson-Delmotte (2006), Ice sheets and sea level, *Science*, *313*, 1043–1045, doi:10.1126/science.313.5790.1043c.

Otto-Bliesner, B. L., S. Marshall, J. T. Overpeck, G. Miller, and A. Hu (2006), Simulating Arctic climate warmth and icefield retreat in the last interglaciation, *Science*, *311*, 1751–1753, doi:10.1126/science.1120808.

Overpeck, J. T., B. L. Otto-Bliesner, G. H. Miller, D. R. Muhs, R. B. Alley, and J. T. Kiehl (2006), Paleoclimatic evidence for future ice-sheet instability and rapid sea-level rise, *Science*, *311*, 1747–1750, doi:10.1126/science.1115159.

Petit, J. R., et al. (1999), Climate and atmospheric history of the past 420,000 years from the Vostok ice core, Antarctica, *Nature*, *399*, 429–436, doi:10.1038/20859.

Radić, V., and R. Hock (2010), Regional and global volumes of glaciers derived from statistical upscaling of glacier inventory data, *J. Geophys. Res.*, *115*, F01010, doi:10.1029/2009JF001373.

Saher, M. H., F. Rostek, S. J. A. Jung, E. Bard, R. R. Schneider, M. Greaves, G. M. Ganssen, H. Elderfield, and D. Kroon (2009), Western Arabian Sea SST during the penultimate interglacial: A comparison of U37K′ and Mg/Ca paleothermometry, *Paleoceanography*, *24*, PA2212, doi:10.1029/2007PA001557.

Sime, L. C., E. W. Wolff, K. I. C. Oliver, and J. C. Tindall (2009), Evidence for warmer interglacials in East Antarctic ice cores, *Nature*, *462*, 342–345, doi:10.1038/nature08564.

Turney, C. S., and R. T. Jones (2010), Does the Agulhas Current amplify global temperatures during super-interglacials?, *J. Quaternary Sci.*, *25*, 839–843, doi:10.1002/jqs.1423.

Vermeer, M., and S. Rahmstorf (2009), Global sea level linked to global temperature, *Proc. Natl. Acad. Sci. U. S. A.*, *106*, 21,527–21,532, doi:10.1073/pnas.0907765106.

Weldeab, S., R. R. Schneider, and P. Müller (2007), Comparison of Mg/Ca- and alkenone-based sea surface temperature estimates in the fresh water–influenced Gulf of Guinea, eastern equatorial Atlantic, *Geochem. Geophys. Geosyst.*, *8*, Q05P22, doi:10.1029/2006GC001360.

Yin, J., J. T. Overpeck, S. T. Griffies, A. Hu, J. L. Russell, and R. J. Stouffer (2011), Different magnitudes of projected subsurface ocean warming around Greenland and Antarctica, *Nat. Geosci.*, in press.

N. P. McKay and J. T. Overpeck, Department of Geosciences, University of Arizona, Tucson, AZ 85721, USA. (nmckay@email.arizona.edu)

B. L. Otto-Bliesner, National Center for Atmospheric Research, Post Office Box 3000, Boulder, CO 80307, USA.